HYPERSPECTRAL REMOTE SENSING FOR MONITORING SPECIES-SPECIFIC DROUGHT IMPACTS IN SOUTHERN CALIFORNIA

by

Austin Reece Coates

A thesis submitted to the faculty of
The University of Utah
in partial fulfillment of the requirements for the degree of

Master of Science

Department of Geography

The University of Utah

December 2015

The University of Utah Graduate School

STATEMENT OF THESIS APPROVAL

The thesis of **Austin Reece Coates**

has been approved by the following supervisory committee members:

Philip Dennison, Chair **5/13/2015**
Date Approved

Dar Roberts, Member **5/15/2015**
Date Approved

Mitchell Power, Member **5/13/2015**
Date Approved

and by **Andrea Brunelle**, Chair/Dean of

the Department/College/School of **Geography**

and by David B. Kieda, Dean of The Graduate School.

ABSTRACT

A drought persisting since the winter of 2011-2012 has resulted in severe impacts on shrublands and forests in southern California, USA. Effects of drought on vegetation include leaf wilting, leaf abscission, and potential plant mortality. These impacts vary across plant species, depending on differences in species' adaptations to drought, rooting depth, and edaphic factors. During 2013 and 2014, Airborne Visible Infrared Imaging Spectrometer (AVIRIS) data were acquired seasonally over the Santa Ynez Mountains and Santa Ynez Valley north of Santa Barbara, California. To determine the impacts of drought on individual plant species, spectral mixture analysis was used to model a relative green vegetation fraction (RGVF) for each image date in 2013 and 2014. A July 2011 AVIRIS image acquired during the last nondrought year was used to determine a reference green vegetation (GV) endmember for each pixel. For each image date in 2013 and 2014, a three-endmember model using the 2011 pixel spectrum as GV, a lab nonphotosynthetic vegetation (NPV) spectrum, and a photometric shade spectrum was applied. The resulting RGVF provided a change in green vegetation cover relative to 2011. Reference polygons collected for 14 plant species and land cover classes were used to extract the RGVF values from each date. The deeply rooted tree species and tree species found in mesic areas appeared to be the least affected by the drought, whereas the evergreen chaparral showed the most extreme signs of distress. Coastal sage scrub had large seasonal variability; however, each year, it returned to an RGVF value only slightly

below the previous year. By binning all the RGVF values together, a general decreasing trend was observed from the spring of 2013 to the fall of 2014. This study intends to lay the groundwork for future research in the area of multitemporal, hyperspectral remote sensing. With proposed plans for a hyperspectral sensor in space (HyspIRI), this type of research will prove to be invaluable in the years to come. This study also intends to be used as a benchmark to show how specific species of plants are being affected by a prolonged drought. The research performed in this study will provide a reference point for analysis of future droughts.

TABLE OF CONTENTS

LIST OF FIGURES

INTRODUCTION

In 2013 and 2014, California experienced one of the worst prolonged droughts in recorded history. On January 1, 2014, Governor Jerry Brown of California declared a drought state of emergency. He stated that due to the current drought in California, residents must be prepared for the possible extreme consequences a lack of water may impose. Some of these consequences include substantial loss in water for agricultural community uses and an increased fire risk in both rural and urban environments ("Governor Brown Declares Drought State of Emergency," 2014). On September 30, 2014, the California Department of Water Resources recorded the third driest water year in the past 119 years with a statewide aggregated precipitation of 30.7 cm. Drought in 2014 followed 2013, in which a statewide aggregated precipitation of only 17.8 cm was reported (California Department of Water Resources, 2014). From July 2014 to October 2014, the National Drought Mitigation Center reported that 58% of California fell within the “Exceptional Drought” category (the most extreme category within their ranking system) and roughly 95% of the state fell within the “Severe,” “Extreme,” or “Exceptional” categories (National Drought Mitigation Center, 2015).

There are many different ways in which to categorize drought and concurrently observe and monitor it, but one of the most visually distinct, and direct, approaches is through the observation of vegetation response. Drought can affect vegetation through a reduction in cell size (Hsiao, 1973), promoting an increase in abscission of leaves and fruit (Jones, 2013), or through plant die back or die off (Davis, Ewers, Sperry, Portwood, Crocker & Adams, 2002; Kolb & Davis, 1994; Parsons, Rundel, Hedlund, & Baker, 1981). Many plant species in southern California shrublands have adaptations to drought. Coastal sage scrub species are often called drought deciduous, in which leaves drop or curl during periods of high water stress. Many evergreen chaparral taxa have rigid leaves that are reinforced with sclerenchyma. This rigid leaf structure helps to protect the plant from the loss of energy associated with leaf repair after wilting (Quinn & Keeley, 2006), thus providing the common observer with few clues as to when these plants are under water stress. Under severe drought stress, many of these plants can self-prune (Quinn & Keeley, 2006), shedding some leaves to allow the whole plant to survive. This type of behavior is prevalent during times of severe drought (Davis et al., 2002; Kolb & Davis, 1994; Parsons et al., 1981) and thus provides the opportunity to observe the impact of drought severity on many of these plant species.

It has been predicted that in the coming years, there will be warmer, longer, and more frequent droughts in many regions of the world (Parry, 2007). California has shown some of the precursors to this trend where there have been gradual increases in temperature (Office of Environmental Health Hazard Assessment, 2013). Year-to-year annual precipitation in this part of the United States varies dramatically, with short and long stretches of both wet and dry years. It has been noted that these shifts in precipitation have no apparent trend (Office of Environmental Health Hazard Assessment, 2013). Despite these large variations in precipitation, the increase in temperature is potentially worsening the effects of the drought conditions. In a study conducted by Van Mantgem and Stephenson (2007) in the Sierra Nevada of California over a 22-year period (1983-2004), both dominant taxonomic groups (*Abies* and *Pinus*) showed an increase in overall mortality rate. This was correlated with a climatic water deficit, which was used as a proxy for a drought index; it had the added value of combining temperature and precipitation into a drought indicator.

Chaparral is a plant community characterized by evergreen sclerophyllous shrubs that are adapted to winter rain and summer drought (Narvaez, Brosh, & Pittroff, 2010). Multiple years of drought could result in a reduction or elimination of nonsprouting species from mixed chaparral communities, and if this loss of biodiversity does occur, then there is the risk of having a shift in community structure and possible desertification (Paddock et al., 2013). It is for this reason that drought monitoring at a species level is important. With a greater understanding of what role drought plays on specific vegetation types, we can begin to plan for future changes in ecosystem function.

This study attempts to quantify the relative percent area in each pixel of the image covered by green vegetation (GV), soil, and nonphotosynthetic vegetation (NPV). By comparing these fractions during a prolonged drought, it was possible to quantify the extent of changes in chaparral canopies on a per species basis. I was able to demonstrate that there was a significant drop in the relative green vegetation fraction (RGVF) associated with severe drought conditions. Presumably, many chaparral species were responding to drought conditions by self-pruning. Through my research, I have demonstrated that changes in RGVF were species-dependent.

BACKGROUND

Effects of Drought on Plants

It is difficult to generalize the effects of drought on all species of plants because each plant species has a different capacity for stress mitigation. Some plants do very well with little water (xerophytes), whereas others can go only a few days without adequate water (hygrophytes). However, even mild stress can affect the growth rate of vegetation in general because cell enlargement is particularly sensitive to drought conditions (Hsiao, 1973). With a lack of water, there is a tendency for stoma to contract. This contraction leads to a reduction in photosynthesis, CO2 uptake, and water loss through evapotranspiration. Many of the plants examined in this study fall under the drought-tolerant category, meaning that they have mechanisms to help them survive and reproduce in drought conditions (Jones, 2013). However, there is no standardized mechanism for how a plant should react to drought. For example, if we were to look only at chaparral communities, all these plants can be considered drought-tolerant with a mix of evergreen and deciduous species coexisting in the same area (Parsons, 1976). Evergreen species tend to have a smaller leaf area-to-mass ratio, lower photosynthetic rates per unit mass, and lower leaf nutrition content, whereas the deciduous species are the exact opposite (Miller, 1981; Mooney & Dunn, 1970). Many of the plant species within California chaparral have root systems that extend both vertically and horizontally. The deep penetrating roots are more suited to drought-prone summer months when the surface water is more scarce; however, when surface water is present, the lateral system takes advantage of the surficial moisture (Cannon, 1911). Some of these deep-rooted, wide lateral spread root system plants include *Arctostaphylos glandulosa*, *Quercus berberidifolia*, and *Quercus chrysolepis* (Hellmers, Horton, Juhren, & O'keefe, 1955). Through excavation, Hellmers et al. (1955) showed that plants can also adapt to their surroundings by altering their root depth to lateral length ratio. In Hellmers et al. (1955), several *Eriogonum fasciculatum* plants were extracted. In one case, the roots extended roughly 1.2 m deep and 0.75 m laterally. In another instance, all of the bulk of the roots stopped at the soil-rock interface, but the plant had lateral roots up to 1.5 m. In yet another case, all of the roots were present in the first 15 cm of soil. With the presence of deep roots, a plant is able to draw on the water deep in the ground while taking advantage of the warm temperatures and high light. In contrast, some species such as *Ceanothus crassifolius* and *Cercocarpus betuloides* have shallow roots (Hellmers et al., 1955) that allow them to use the autumn rain and allocate more carbohydrates to aboveground growth (Ackerly, 2004). Although these plant species have varied mechanisms that allow them to withstand some drought conditions, in cases of extreme or prolonged drought, the physiological adaptations of these species may not be sufficient.

For example, if water potential, which indicates the ability of the water inside one cell to move to another cell, drops below a certain level (e.g., -4.5 MPa for *Salvia mellifera* and -11 MPa for *Ceanothus megacarpus* (Kolb & Davis, 1994)), woody plants may begin to form small air bubbles (emboli). These emboli are formed through cavitation in their xylem (the tissue that transports water throughout the plant) and tracheids, which can potentially cause water transport blockages or embolism (Kolb &

Davis, 1994). An embolism within the xylem has been linked to leaf drop in coastal sage scrub and die back in chaparral (Davis et al., 2002; Kolb & Davis, 1994; Paddock et al., 2013). Leaf senescence and abscission are what make up the main changes in percent green vegetation cover in the current study region. Sclerenchyma in evergreen chaparral taxa enables these species to experience very little wilting even though many of these plans have very efficient stoma closure mechanisms (Miller, 1979; Poole & Miller, 1975)

Remote Sensing of Drought

One of the earliest examples of drought monitoring from satellite data was using data from the Advanced Very High Resolution Radiometer (AVHRR). With the availability of red and near infrared (NIR) bands, it was possible to see NIR scattering and variations in chlorophyll absorption; however, chlorophyll saturates quickly so this method has limited viability. This method was used to derive plant health on a global scale. Red and near infrared bands allow calculation of the Normalized Difference Vegetation Index (NDVI), used by many studies to examine drought impacts on vegetation. Peters et al. (2002) used the NDVI to monitor drought over the central United States during a 12-year period. Rahimzadeh Bajgiran, Darvishsefat, Khalili, and Makhdoum (2008) showed that through the use of vegetation indices and the NDVI, they could monitor drought in northwest Iran over a 5-year period. Drought monitoring has also been performed on a finer spatial scale with the use of instruments such as Landsat and Satellite Pour l'Observation de la Terre (SPOT) (Aguilar, Zinnert, Polo, & Young, 2012; G. P. Asner & Alencar, 2010; Vogelmann, Tolk, & Zhu, 2009). When using these sensors, many of the researches opted to use NDVI differencing as their main analysis tool because these sensors are multispectral sensors and do not possess the spectral resolution to perform finer scale spectroscopy.

G. P. Asner et al. (2003) noted that fine-resolution drought monitoring required greater spectral resolution than can be obtained by Landsat, SPOT, AVHRR, and Moderate Resolution Imaging Spectroradiometer (MODIS). G. P. Asner et al. (2003) used narrowband vegetation indices (NDVI, Simple Ratio (SR), Normalized Difference Water Index (NDWI), Photochemical Reflectance Index (PRI), Anthocyanin Reflectance Index (ARI)), and the EO-1 Hyperion sensor to monitor drought impacts on tropical forests. Claudio et al. (2006) showed that through the use of the NDVI and the water band index (WBI) derived from AVIRIS imagery, subtle variations in specific plant species can be observed. It was inferred through the use of the NDVI that there was a change in green vegetation due to drought conditions, which was later confirmed through fieldwork.

The approach of using spectral mixture analysis was demonstrated in Huang and Anderegg (2012), who showed that it is possible to use a spectral mixture analysis of NPV and photosynthetic vegetation endmembers to monitor drought. However, in Huang and Anderegg (2012), a multispectral sensor was used, which hindered them from seeing subtle differences in specific plant species. D. A. Roberts, Dennison, Peterson, Sweeney, and Rechel (2006) also showed that it was possible to monitor changes in plant health, specifically within the chaparral community, from airborne/space-borne platforms. D. A. Roberts et al. (2006) used fractional changes in GV and NPV that were derived from an extensive time series of AVIRIS and MODIS imagery through the use of spectral mixture analysis as indicators of change in live fuel moisture (LFM). They showed that fractional changes in GV and NPV were good indicators of change in fuel below a cutoff of 60% LFM. This result shows it is possible to use SMA to see variations in plant health of a Mediterranean climate over a long temporal scale from an airborne sensor. In D. Roberts, Green, and Adams (1997), it was also shown that SMA is an effective method for monitoring changes in vegetation, and by using appropriate reference endmembers, it is possible to accurately see seasonal changes in GV. The progression of these studies gives credence to the hypothesis that it is possible to perform species-specific drought monitoring by using spectral mixture analysis and hyperspectral imaging. Although previous studies have laid the groundwork for this type of analysis, these methods have yet to be combined for the purpose of drought monitoring to the best of the author's knowledge. Therefore, this study provides new insight into the ecological impacts of drought and creating new methods for monitoring vegetation at the species level.

Hyperspectral Remote Sensing

Hyperspectral remote sensing instruments collect data in hundreds of different wavelengths/bands. Due to the way in which the instruments are designed, they can measure narrow ranges of wavelengths within the electromagnetic spectrum. By having narrow bands, it is possible to distinguish small features within spectral responses more easily (Ustin, Roberts, Gamon, Asner, & Green, 2004). For example, the Airborne Visible InfraRed Imaging Spectrometer (AVIRIS) is an airborne hyperspectral sensor that can collect 224 contiguous 10 nm wide bands with wavelengths ranging from 350 to 2500 nm. AVIRIS has the ability to be flown on a variety of different platforms, including NASA's ER-2 jet and Twin Otter International's turboprop. An example of the advantages of having a large number of bands can be seen in Dennison and Roberts (2003), where they used AVIRIS imagery along with multiple endmember spectral mixture analysis (MESMA) and endmember average root mean square error to map land cover, including four dominant vegetation species, soil, and senesced grass, in the Santa Ynez Mountains above Santa Barbara, California. Fine spectral resolution is necessary to discriminate between NPV and soil using absorption features of lignin and cellulose (G. Asner & Heidebrecht, 2002; Roberts, 1993).

Linear Mixture Modeling Approach

Previous studies have demonstrated that an effective way in which to extract the fractional cover of a specific material in a landscape is to model the spectral characteristics of each pixel individually (Jensen, 2005). A common way in which to represent the amount of photosynthetic biomass in an area, and/or the leaf area index (LAI), is through the use of the NDVI (Diallo, Diouf, Hanan, Ndiaye, & Prevost, 1991; Gilabert, Gandía, & Meliá, 1996; Hobbs, 1995; Jensen, 2009; Tucker, Justice, & Prince, 1986; Tucker, Vanpraet, Sharman, & Van Ittersum, 1985). However, using a single NDVI value per pixel, which is often used as a proxy for plant health, can sometimes lead to an incomplete understanding of the physical phenomena that are occurring within that pixel. Linear mixture modeling (also known as spectral mixture analysis or SMA) is a method that has been shown to more easily differentiate specific spectral features associated with GV, NPV, and soil with a mixed pixel. In this approach, it is assumed that each pixel being imaged is made up of multiple materials, and to accurately model the fractional amount of each material, the target spectra must be decomposed. SMA uses linear combinations of endmembers, or pure spectra that have been collected in the field, from the image, or in the laboratory to model the spectra in question. The resulting model contains the fractional amounts of each endmember that were used to model the target spectra. A spectral reflectance (p'_{λ}) can be modeled with fractional amount (f_i) of the endmember i at wavelength λ with a residual error of ε_{λ}, where N is the number of endmembers (Dennison & Roberts, 2003).

$$p'_{\lambda} = \sum_{i=1}^{N} f_i * p_{i\lambda} + \varepsilon_{\lambda} \tag{1}$$

SMA has been widely used in the literature to calculate the fractional abundance of endmembers within a mixed pixel. McGwire, Minor, and Fenstermaker (2000) showed that by using a linear spectral mixture model, they could more accurately identify sparse vegetation in arid environments as compared to using vegetation indices. Huang and Anderegg (2012) showed that it is possible to monitor aspen forest health in the Rocky Mountains as a result of drought by looking at the fractional amounts of aboveground biomass as compared to nonphotosynthetic vegetation derived from linear spectral unmixing. D. A. Roberts et al. (1998) used a derivative of SMA called Multiple Endmember Spectral Mixture Analysis (MESMA) to map chaparral communities in the Santa Monica Mountains. They did this through varying the endmember that represented GV, NPV, and soil in each pixel, and then picking the optimal model based on a set of parameters. The resulting map shows the fraction amount of GV, NPV, and soil in each pixel in addition to the endmember that modeled those fractions. Although MESMA is an attractive possibility for use in this research, simple SMA will be used because it is important that endmembers remain identical for each pixel over time to allow for comparison of endmember fractions over time.

Multitemporal time series analysis in conjunction with SMA is not a completely unique method. For example, it has previously been used for species-specific mapping (Somers & Asner, 2014). However, in this study, SMA was used to look at fractional differences in endmember abundance not as it relates to drought, but rather how it relates to species mapping. Somers and Asner (2014) used a modified version of MESMA called Wavelength Adaptive Spectral Mixture Analysis (WASMA) in addition to a six-image hyperspectral time series to improve on vegetation mapping. The changes in spectral characteristics from scene to scene helped to create separability between the different plant species spectra, which aided in the mapping of the different taxa. This study and previous studies (Somers & Asner, 2012; Somers & Asner, 2013) help to illustrate the point that there is valuable spectral information in hyperspectral time series. Also, through the use of SMA, it is possible to tease out subtle variations in the data that can be used to evaluate plant taxa. Somers and Asner (2014) showed that variation in spectra could be used to advantage in differentiating spectra; however, in the current study, it is not the goal to quantify the differences in terms of environmental impact but rather in terms of spectral variability. It is for this reason that WASMA will not be used directly but rather as illustration of what can be done with a multitemporal hyperspectral image stack. Röder et al. (2009) demonstrate a test case that is more similar to the study currently being presented, which uses SMA to evaluate the impacts of changes in grazing practices in the Lagadas County of Greece. Through the use of SMA, Röder et al. (2009) were able to extract the fractional amount of green vegetation in each pixel and look at the changing amounts from year to year. Statistical modeling was then used to better understand the various feedbacks present in the watershed of the Mygdonia Valley in northern Greece.

METHODS

Study Area

This study was performed in and around Santa Barbara, California. The study area runs from the Pacific Ocean up through the Santa Ynez Mountains and then further north into the San Rafael Mountains; the geographical extent can be seen in Figure 1. Included in the study area are farmlands, rural and urban areas, and some of the coastline. Santa Barbara County averages about 46.7 cm of rain annually, with the majority of it occurring between October and April (National Oceanic and Atmospheric Administration (NOAA), 2014). This region has moderate temperatures that are cool and wet in the winter and warm and dry in the summer, typical of a Mediterranean climate.

For this study, AVIRIS data collects in 2011, 2013, and 2014 were used. These dates were chosen because they show what conditions were like in the region before 2011 and the 2013-2014 drought. Figure 2 shows how precipitation in Santa Barbara changed from 2011 to 2013.

Reference Data

Roth, Dennison, and Roberts (2012) collected reference data during field campaigns. An adaptation of Meentemeyer and Moody's (2000) composition estimation method was used for data collection. A high-powered spotting scope was used to collect information about patches of dominant plant species and their relative composition.

Patches that had more than 75% agreement with a single class were then digitized on an AVIRIS flight line. See Table 1 for specific reference information about the species, acronyms, functional type, and number of pixels used per date in this study.

Imagery Data

The NASA Jet Propulsion Laboratory (JPL) collected the imagery that was used for this project with the AVIRIS sensor. AVIRIS was flown over the Santa Barbara study area once in 2011 (July 19th), four times in 2013 (April 11th, June 6th, November 25th, December 4th), and four times in 2014 (April 16th, June 4th, June 6th, August 29th). The sensor was flown at an altitude of roughly 14 km in 2011 and 20 km in 2013/14 onboard a NASA ER-2 aircraft. This instrument orientation resulted in a spatial resolution of 15.9 m for 2013/14 and a 6.8 m for 2011. During each flight, AVIRIS collected 224 contiguous bands of spectral data with a bandwidth of 10 nm and wavelengths ranging from 350 to 2500 nm.

Preprocessing Methods

All imagery used in this study was converted to apparent surface reflectance. To convert the data to surface reflectance, the Atmosphere Removal Algorithm (ATREM) was used to correct for atmospheric effects (Thompson et al., 2014) NASA JPL performed this step in addition to resampling the data to a spatial resolution of 18 m. The remaining water absorption features were then manually selected and discarded. In order to perform analysis of the images, each scene was geo-referenced by hand, and then a mosaic of each date was created and clipped to the common extent of all the years.

Endmember Selection Method

In order to extract relative fractional land cover on a per pixel basis, linear spectral unmixing was performed, with three endmembers: shade, GV, and NPV. This three-endmember model was used to model each of the image pixels, thus producing a set of images in which each image represents the relative fractional amount of each endmember as compared to 2011-07-19. The way in which the GV endmembers were selected was by first thresholding the 2011-07-19 image to isolate only those areas with an NDVI value greater than 0.3. This threshold of 0.3 was determined by comparing the cumulative distributions of NDVI values with respect to predominately green vegetation reference polygons (ADFA, ARCASALE, ARGL, CECU, CEME, CESP, ERFA, EUSP, PISA, PLRA, QUAG, QUDO, UMCA) and nongreen vegetation reference polygons (rock, soil, agricultural residues). The selected NDVI threshold captured 95% of the GV reference pixels and only 12% if the non-GV reference pixels. It is possible to exclude more non-GV reference pixels, but that would have meant fewer of the GV reference pixels were available for analysis, which was undesirable for this study (Figure 3). All reference pixels with an NDVI value greater than 0.3 were used as the GV endmember for that pixel only. A photometric shade endmember was made up of all zero values. For the remaining NPV endmember, a single lab spectrum was used (Roberts et al., 1999; Dennison & Roberts, 2003).

In a previous study that also used SMA to model subpixel groundcover (McGwire et al., 2000), GV, soil, and shade endmembers were used, whereas we substituted an NPV endmember for soil. This NPV endmember was substituted because in drought situations, many plants produce small and/or fewer leaves or die off completely. This reduction in leaf area and increase in NPV, by way of more branches being exposed in addition to dead leaves, was one of the main indicators of plant stress in this study. By using these three endmembers, it was possible to more accurately model the landscape.

Once all the pixels in the image were modeled, shade normalization was performed. Shade normalization is performed by dividing the fraction of each nonshade endmember by the sum of the nonshade endmembers (Adams & Gillespie, 2006). Shade normalization removed some of the effects caused by viewing/solar geometry and topography, which reduced errors when comparing scenes from different dates and times.

The reference polygons were used to extract information about each species. Since each reference polygon had been previously labeled with the dominant species/landcover type contained within it, it was only a matter of extracting the fractional changes of relative GV and NPV within these classified pixels in order to determine species level changes.

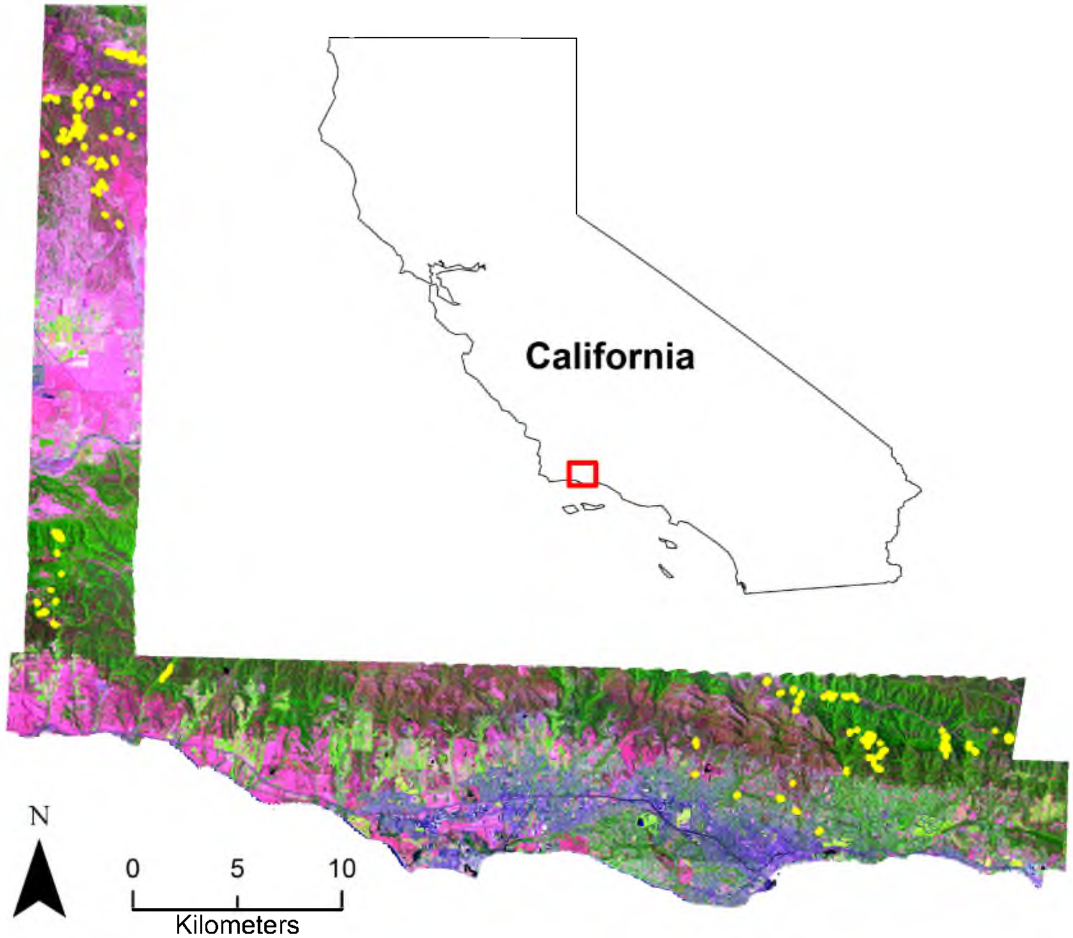

Figure 1. The study region covering the Santa Barbara Coast and portions of the Santa Ynez Mountains and Santa Ynez Valley, California. An AVIRIS images acquired in July 2011 is shown in a 1651 nm (red), 831 nm (green), 658 nm (blue) false color composite. Reference polygons dominated by plant species are marked by yellow dots.

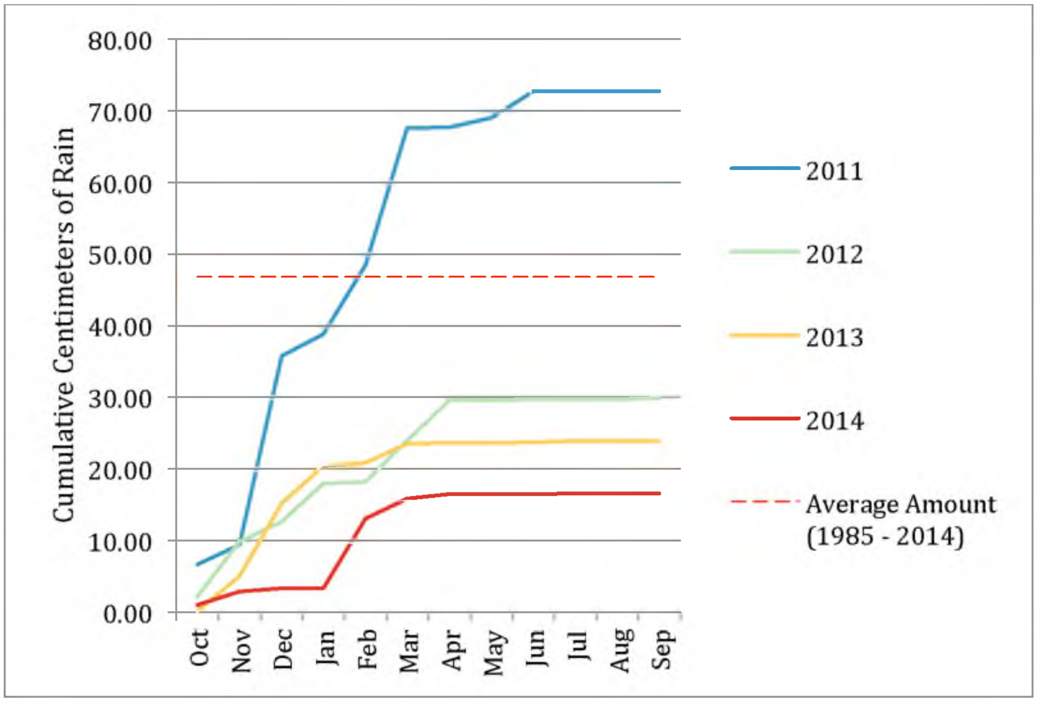

Figure 2. Cumulative rain in Santa Barbara, California from Oct. 2011-Sep. 2014 (National Oceanic and Atmospheric Administration (NOAA), 2014).

Table 1. Species, Acronyms, Functional Type, and Number of Pixels Used Per Date

Type	Code	Functional Type	N Pixels
Adenostoma fasciculatum	ADFA	Evergreen Chaparral	2688
Artemisia californica /Salvia leucophylla	ARCA-SALE	Coastal Sage Scrub	210
Arctostaphylos glauca/glandulosa	ARGL	Evergreen Chaparral	342
Baccharis pilularis	BAPI	Evergreen Chaparral	255
Brassica nigra	BRNI	Forb	72
Ceanothus cuneatus	CECU	Evergreen Chaparral	318
Ceanothus megacarpus	CEME	Evergreen Chaparral	720
Ceanothus spinosus	CESP	Evergreen Chaparral	960
Eriogonum fasciculatum	ERFA	Coastal Sage Scrub	210
Mediterranean Annual Grass/Forb	MAGF	Annual Grasses	1470
Pinus sabiniana	PISA	Native Tree Species	1230
Platanus racemosa	PLRA	Native Tree Species	672
Quercus agrifolia	QUAG	Native Tree Species	1170
Quercus douglasii	QUDO	Native Tree Species	2835
Umbellularia californica	UMCA	Native Tree Species	216

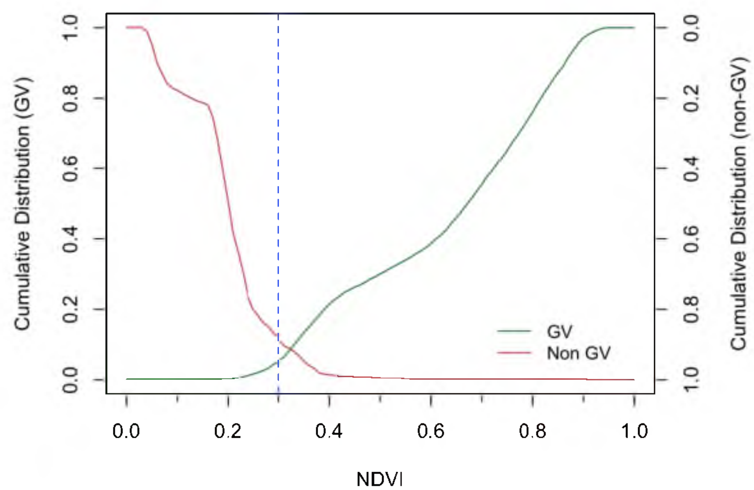

Figure 3. NDVI threshold selection through the use of GV and non-GV reference pixel cumulative distributions.

RESULTS

Figure 4 demonstrates the fractional changes in green vegetation cover as compared to 2011-07-19. A yellow color in Figure 4 indicates that the pixel in question was spectrally very similar to the corresponding 2011-07-19 pixels and was modeled with a near 1 to 1 fractional GV cover value. Since the scenes have been masked to include only those pixels with higher than 0.3 NDVI values, a green color pixel can be interpreted as an increase in GV whereas a red color is mapped to those values that indicate a loss in GV

An increase in relative green vegetation fraction (RGVF) is present in the lower elevation coastal sage scrub, as can be seen in row B of Figure 5. This increase in RGVF is consistent with the seasonal variability of the coastal sage scrub that is present in that portion of the study area. The reason there is such a large change in RGVF, when comparing spring 2013/2014 to the 2011 reference image, is the greenup of these species in the early spring as compared to the later collection date of the 2011 image. Another increase in RGVF can be seen in row C of Figure 5, which shows the higher elevations and subsequent regrowth after the 2008 Gap Fire. As for the other higher elevations, there is little change in GV as compared to 2011 other than the seasonal variability, which is being amplified by the lack of precipitation. One area in the image that seems to be impervious to the drought is located along the long northern stretching flight line (refer to row A of Figure 5 and Figure 4). Roughly halfway up this flight line, in the city of Santa

Ynez, there are several farms and stables that seem to always be green, which is what we would expect to see in an area that relies on irrigation.

Year-to-year variability is captured by looking at only those pixels that fall within the reference polygons, more specifically, only the pixels within that set that had an NDVI value of 0.3 or greater. All plots in Figure 6 and Figure 7 have been offset along the y-axis for ease of visualization. Figure 5 shows a negative trend in RGVF values from 2013-04-11 to 2014-8-29. There is a small amount of green up occurring in the spring of 2014, but it falls below the levels of spring 2013, which is a result of the stress of the previous year's drought conditions and the continuing drought conditions in 2014. This negative trending can also be seen in Figure 6.

In Figure 7, the data are broken down even further into individual plant species. The species in this figure can be grouped into three broad classes: evergreen chaparral, grasslands and coastal sage scrub, and native trees. Evergreen chaparral tends to be more visibly drought tolerant and have a tighter distribution of RGVFs. Grasses and coastal sage scrub are seasonally senescent and/or drought deciduous, thus creating large swings in their GV distribution plots. The trees have deep roots and tend to show fewer signs of seasonal variability. The species that fall into the evergreen chaparral class are ADFA, ARGL, BAPI, CECU, CEME, and CESP. ARCA-SALE and ERFA are within the coastal sage scrub group, and MAGF and BRNI are annual grasses and forbs, respectively. The remaining species are PISA, PLRA, QUAG, QUDO, and UMCA, which are all native tree species.

Within the evergreen chaparral group, there is a general trend of tighter distributions and small shifts in green vegetation from year to year and season to season.

However, there are exceptions to the rule. For example, BAPI, which is an evergreen shrub that can be considered part of the coastal sage scrub or the evergreen chaparral, shows a short resurgence in GV on 2013-11-25, which is consistent with its blooming cycle of August to November (Dale, 1986). The blooming of BAPI is apparent to some extent in 2014; however, the imagery was collected earlier in the year and the drought may also have played a role in the subdued signal. It is interesting to note that CECU, CEME, and CESP are the same genus but react very differently to the prolonged drought. CESP showed significant die off or senescence and subsequent regrowth from 2013 to 2014, whereas CECU and CEME have both steadily declined. It is also interesting to note the distribution of GV cover in the CECU pixels as compared to the CEME. CECU has a much wider spread of RGVF values, indicating that canopy cover is much more diverse for that species as compared to CEME.

The coastal sage scrub species, annual grasses, and forbs have a very similar distribution to that of CECU. In some instances, the distribution is even more dispersed (e.g., ARCA-SALE). An extreme example of this is ARCA-SALE in 2013-11-25. The values for each bin of the distribution were so similar that at the resolution of this plot, it appears almost as though there is no variation between relative fractional cover, due in part to much of the area being covered in 2011 by healthy green ARCA-SALE, whereas in 2013 and 2014, this area has been decimated by the drought, leaving very little GV behind. This major reduction in GV across all ARCA-SALE polygons is what gives that flat elongated distribution. Of all classes in the coastal sage scrub group, ERFA has the most dramatic variations in the placements of its distributions. A potential explanation for this is that ERFA might only partially cover the target pixels and has a greater amount of subdominant cover of more drought-sensitive, herbaceous species than the other species within the coastal sage scrub group. On the other hand, 2013-04-11 was collected right during the growth period, and therefore shows a large positive GV fraction; this is also the case for 2014-04-16.

When comparing the native tree class to the other classes, it becomes apparent that there is something different about how arboreal species deal with drought. There is still a negative trend in the RGVF distributions; however, the rate of this change is much slower and is less pronounced. QUAG is an example of a species that is showing little or no change in RGVF. However, it is noteworthy that two species from the same genus can react so differently to drought conditions. When comparing QUAG and QUDO, it can be seen that these two species do in fact have very different drought characteristics, which can be explained by the existence of different physical adaptations (Canadell et al., 1996; Hellmers et al., 1955) QUDO is winter deciduous (Pavlik, Muick, Johnson, & Popper, 1991) whereas QUAG is evergreen. Additionally, QUDO has a significant grass understory and has a less dense canopy; the opposite is true of QUAG. These factors result in a more dispersed distribution of RGVF for QUDO, which has a distribution that looks very similar to the other deciduous plants.

One other aspect that can be analyzed with these data is root depth and its effects on plant health during a drought. By ordering the species, QUAG, ADFA, ERFA, CECU, ARCA, from deepest roots to shallowest roots, a pattern can be seen where deeper roots have tighter distributions and less negative RGVF trending whereas the opposite is true for those species with shallower roots.

In an attempt to directly compare dates across all years, one can look at 2013-06-

06 and 2014-06-04. These dates are the closest to the reference image collection date of 2011-07-19. By looking at these dates, it is possible to see a very subtle trend of reduced green up in 2013 and even more so in 2014 in the evergreen chaparral group. Though there is a reduction in GV as compared to 2011, coastal sage scrub is not showing as extreme a reaction to the drought conditions. CECU and CEME are showing more loss in GV compared to ARCA-SALE, which has the highest loss for the coastal sage scrub species. For the native tree species, UMCA is the only one from these dates that has any discernible negative trend in GV.

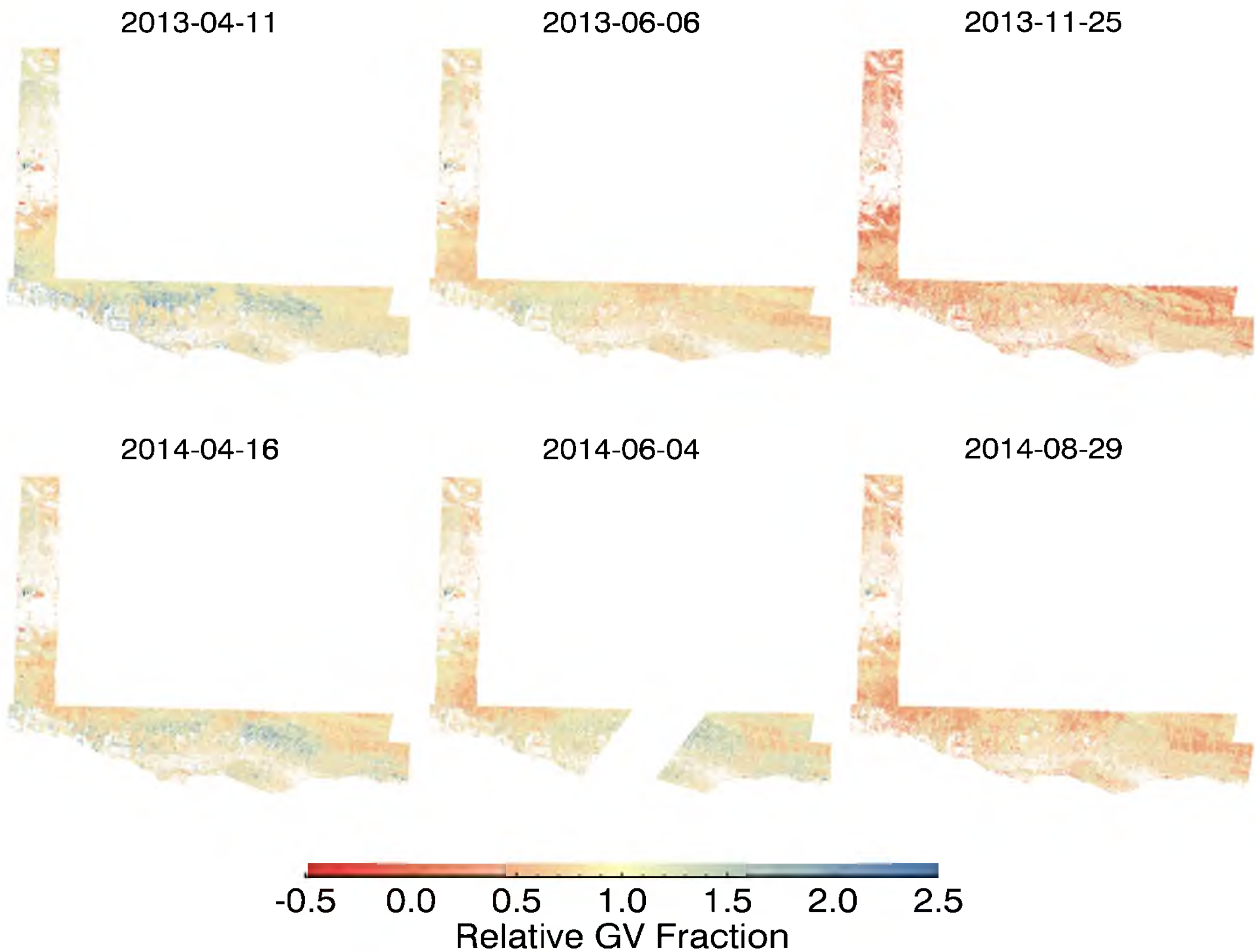

Figure 4. Relative GV fraction for dates in 2013 and 2014. White areas indicate pixels with an NDVI less than 0.3 in the July 2011 data. An instrument malfunction resulted in missing data for the white strip shown in the 2014-06-04 image

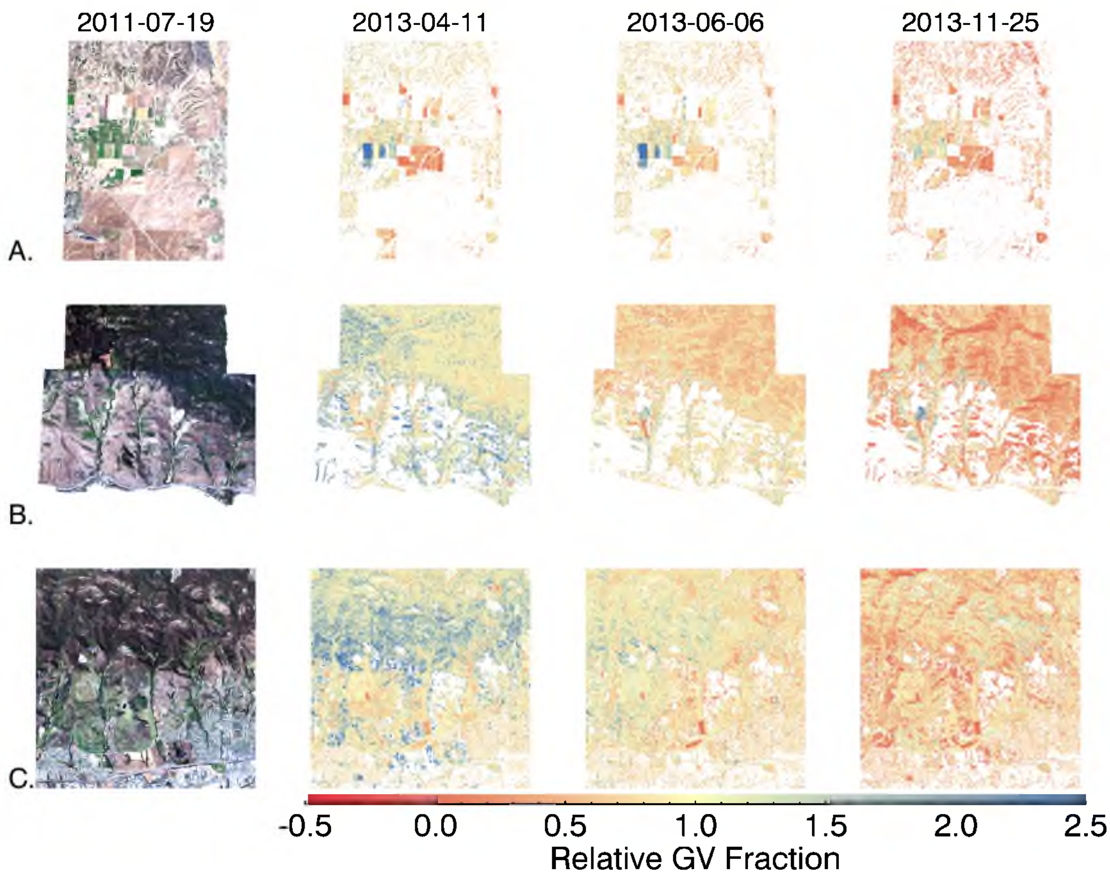

Figure 5. A. Agriculture in the Santa Ynez valley; B. Chaparral (top-right) and coastal sage scrub and grasslands (bottom-left); C. The fire scar of the 2008 Gap fire (top) and agriculture and grasslands (bottom). White areas indicate pixels with an NDVI less than 0.3 in the July 2011 data.

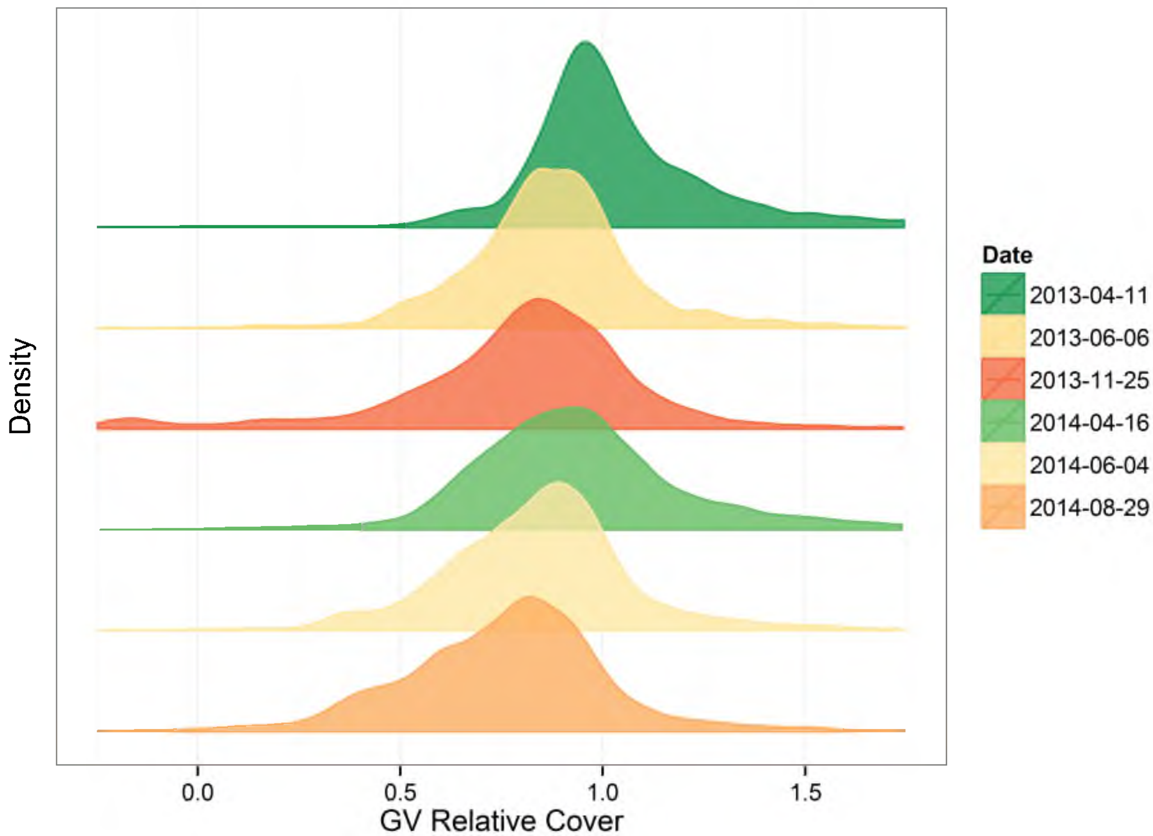

Figure 6. Relative GV cover for all pixels within delineated polygons

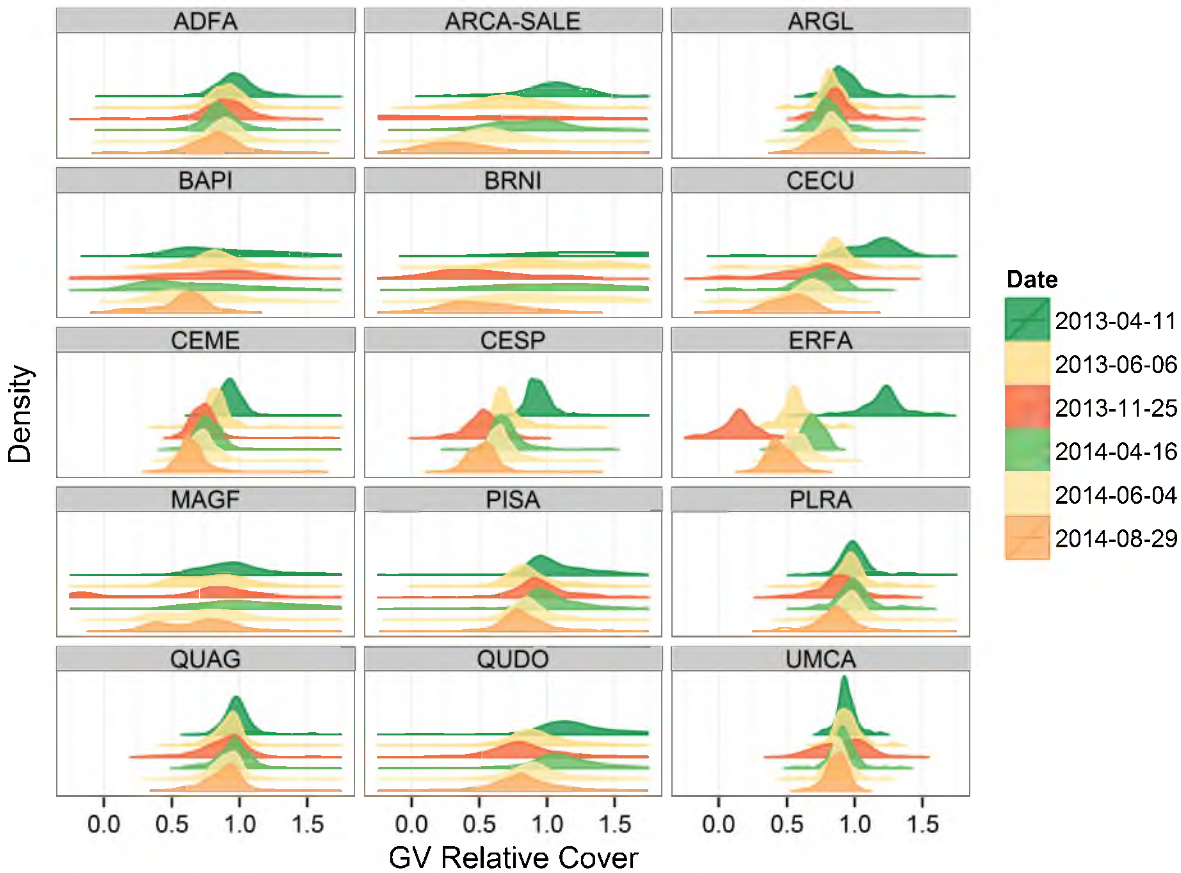

Figure 7. Changes in RGVF on a per pixel and per species basis

DISCUSSION

Each of the species in Figure 7 can be compared with all the other species in the Figure 7, and can also be examined for seasonal variation within itself. These variations represent a gradient of responses from sensitive (e.g., ERFA) to insensitive (e.g., QUAG); however, they exist regardless of the species. It is difficult to say why specific plants have adapted to their environment in the way they have, or why they react the way they do to drought conditions, but through hyperspectral remote sensing, we are able to begin to see large-scale trends and variations. Sometimes these variations are easy to explain and other times they bring up more questions than answers. Once again examining ERFA/QUAG with regard to seasonality, it can be inferred that the large seasonal variability within the ERFA RGVF profile comes from the senescence in the fall and eventual green up in the spring. QUAG, on the other hand, does not senesce in the same way, and for this reason, it does not have this large shift back and forth in GV. This begs the question, which one of these plants is better adapted for surviving the drought? QUAG is showing fewer visible signs of stress but is it depleting more of its carbohydrate reserves, and experiencing something similar to cavitation fatigue, thus hindering its ability to survive a more minor drought in the future (Anderegg et al., 2012)? Or is ERFA gradually diminishing its lifespan through the continual death and regrowth of its leaves, eventually leading to its inability to blossom and reproduce?

A complicating factor in plant health monitoring for many of these species is the existence of multiple plants inhabiting the same pixel. For example, QUDO is winter deciduous and has a prevalent grassy understory. Due to the openness of the canopy when collecting data for this species, mixed pixels are unavoidable. Because of the mixed spectra, it is difficult to tell where one species ends and another begins. This pairing of species distorts the distribution as well, because when QUDO is fully leafed out during the summer months, there is some mixing of the spectra; however, when the leaves drop in the winter, the grass remains and begins providing a RGVF of its own. This swapping of plant species visible within pixels may be what gives the more dispersed distribution and gentle decline in RGVF, rather than a sharp decline.

The intent of this study was to show the impacts of drought on a per species basis. This was accomplished through the use of reference polygons and relative green vegetation fractions. The initial strategy to do this was to use a three-endmember model with the option for the model to change between GV, NPV, and shade; GV, soil, and shade; or NPV, soil, and shade. This approach, however, proved problematic given the fact that shifting between dates caused the model to change as well. When this flipping of the model occurred, it was no longer possible to compare one date to another. I solved this problem by using a fixed NPV endmember and a unique GV endmember for each pixel, which solved the problem of the model flipping back and forth and provided the ability to compare one date to another. In this study, I used an above-average precipitation year and compared it with the two consecutive drought years. This type of methodology provides an alternative to something like MESMA, which can be difficult to apply to multitemporal data sets. MESMA does a wonderful job at classifying imagery as well as calculating fractional ground cover; however, when switching between image dates, it also has problems with models flipping back and forth. By using the method presented in this paper, it is possible to reduce model complexity by forgoing the use of a soil endmember and using only GV and NPV endmembers, in addition to a photometric shade spectrum. By reducing the number of endmembers, the potential for negative fractions is also reduced. One drawback of using a simplified model such as the one employed here is that it is now possible to easily inflate the relative NPV fractions, because there is no longer a means for differentiating NPV from soil. Based on my findings, quantifying the relative fractional amounts of GV was the best way to monitor stress since the goal of this study was to monitor drought stress on specific species of plants. Therefore, it was a logical decision to reduce the complexity of the model while still maintaining the most important variable: GV.

In future research, I would like to include thermal infrared (TIR) imagery in the analysis. Through the use of TIR data, it would be possible to analyze drought on specific plant species with more accuracy. D. A. Roberts, Dennison, Roth, Dudley, and Hulley (2015) recently published a paper comparing hyperspectral data to land surface temperature and in doing so, outlined a method for clustering ground cover types based on their temperatures and GV fractions. In an effort to expand this model that has already been established, future research will be conducted to merge their findings with a multitemporal time series. If I had had access to TIR data in our study, it may have been possible to extract self-clustering of the land cover types instead of user-defined clusters (e.g., evergreen chaparral, coastal sage scrubs, grasses, forbs, and native trees). This research along with higher temporal resolution imagery could be used to create better prediction and monitoring tools that could be used to identify where and when different plant species will succumb to drought conditions.

CONCLUSION

A hyperspectral sensor in space, such as the HyspIRI mission, would provide a unique opportunity for long-term drought monitoring on the species level. The current orbiting systems do not provide the temporal and spectral resolution to perform a long-term study such as the one outlined in this paper. In an attempt to mimic the data products that someday could be produced by the HyspIRI mission, 18m AVIRIS imagery was used to look at the effects of drought on a species level.

A three-endmember linear spectral unmixing model was used to relate the RGVF cover from three scenes in 2013/2014 to a single scene in 2011. The resulting SMA maps showed seasonal variations across the landscape, going from green up in spring to senescence and die back in fall, as well as a general negative trend in RGVF for all species. The native trees of the area showed the smallest change in overall RGVF, whereas the coastal sage scrub group, which senesces in response to seasonal drought, appeared to be affected more severely. The evergreen chaparral species, which reduce their evapotranspiration in response to seasonal drought, were affected most severely. It was also observed that plants with deeper roots (i.e., QUAG, ADFA) had tighter distributions and were less affected by the drought, whereas species with shallower root depths were more severely impacted.

The combination of relatively high temporal resolution and spectral resolution allowed for the possibility not only to look at the GV as a whole, but also to identify specific species and land cover classes within the study area. With the combination of hyperspectral and TIR sensors on board the HyspIRI platform, future research will be possible in linking species type and GV cover to thermal responses caused by drought. This area of research is newly emerging due to limited data resources up to this point; however, with the proposed HyspIRI mission, this type of large-scale, high temporal resolution study will become commonplace in the years to come.

REFERENCES

Ackerly, D. (2004). Functional strategies of chaparral shrubs in relation to seasonal water deficit and disturbance. *Ecological Monographs, 74*(1), 25-44.

Adams, J. B., & Gillespie, A. R. (2006). *Remote sensing of landscapes with spectral images: A physical modeling approach*. Cambridge, UK: Cambridge University Press.

Aguilar, C., Zinnert, J. C., Polo, M. J., & Young, D. R. (2012). NDVI as an indicator for changes in water availability to woody vegetation. *Ecological Indicators, 23*(0), 290-300. doi:http://dx.doi.org/10.1016/j.ecolind.2012.04.008

Anderegg, W. R., Berry, J. A., Smith, D. D., Sperry, J. S., Anderegg, L. D., & Field, C. B. (2012). The roles of hydraulic and carbon stress in a widespread climate-induced forest die-off. *Proceedings of the National Academy of Sciences, 109*(1), 233-237.

Asner, G. P., Nepstad, D., Cardinot, G., Moutinho, P., Harris, T., & Ray, D. (2003). EO-1 hyperion measures canopy drought stress in Amazonia. *AVIRIS Proceedings*.

Asner, G. P., & Alencar, A. (2010). Drought impacts on the Amazon forest: The remote sensing perspective. *New Phytologist, 187*(3), 569-578.

Asner, G. P., & Heidebrecht, K. B. (2002). Spectral unmixing of vegetation, soil and dry carbon cover in arid regions: Comparing multispectral and hyperspectral observations. *International Journal of Remote Sensing, 23*(19), 3939-3958.

California Department of Water Resources. (2014, October 10th, 2014). Water Year 2014 Ends as 3rd Driest in Precipitation. *Breaking Drought News*. Retrieved from http://www.water.ca.gov/waterconditions/

Canadell, J., Jackson, R. B., Ehleringer, J. B., Mooney, H. A., Sala, O. E., & Schulze, E. D. (1996). Maximum rooting depth of vegetation types at the global scale. *Oecologia, 108*(4), 583-595. doi:10.1007/BF00329030

Cannon, W. A. (1911). *The root habits of desert plants* (Vol. 131). Baltimore, MD: Carnegie Institution of Washington.

Claudio, H. C., Cheng, Y., Fuentes, D. A., Gamon, J. A., Luo, H., Oechel, W., . . . Sims, D. A. (2006). Monitoring drought effects on vegetation water content and fluxes in chaparral with the 970 nm water band index. *Remote Sensing of Environment, 103*(3), 304-311.

Dale, N. (1986). *Flowering plants: the Santa Monica Mountains, coastal & chaparral regions of Southern California*. Santa Barbara, CA: Capra Press.

Davis, S. D., Ewers, F. W., Sperry, J. S., Portwood, K. A., Crocker, M. C., & Adams, G. C. (2002). Shoot dieback during prolonged drought in Ceanothus (Rhamnaceae) chaparral of California: A possible case of hydraulic failure. *American Journal of Botany, 89*(5), 820-828. doi:10.2307/4131324

Dennison, P. E., & Roberts, D. A. (2003). Endmember selection for multiple endmember spectral mixture analysis using endmember average RMSE. *Remote Sensing of Environment, 87*(2), 123-135.

Diallo, O., Diouf, A., Hanan, N. P., Ndiaye, A., & Prevost, Y. (1991). AVHRR monitoring of savanna primary production in Senegal, West Africa. 1987-1988. *International Journal of Remote Sensing, 12*(6), 1259-1279.

Gilabert, M. A., Gandía, S., & Meliá, J. (1996). Analyses of spectral-biophysical relationships for a corn canopy. *Remote Sensing of Environment, 55*(1), 11-20.

Governor Brown Declares Drought State of Emergency. (2014, January 17th 2014). *News*. Retrieved from http://www.gov.ca.gov/news.php?id=18368

Hellmers, H., Horton, J., Juhren, G., & O'keefe, J. (1955). Root systems of some chaparral plants in southern California. *Ecology*, volume number, 667-678.

Hobbs, T. J. (1995). The use of NOAA-AVHRR NDVI data to assess herbage production in the arid rangelands of central Australia. *International Journal of Remote Sensing, 16*(7), 1289-1302.

Hsiao, T. C. (1973). Plant responses to water stress. *Annual Review of Plant Physiology, 24*(1), 519-570. doi:10.1146/annurev.pp.24.060173.002511

Huang, C. Y., & Anderegg, W. R. (2012). Large drought-induced aboveground live biomass losses in southern Rocky Mountain aspen forests. *Global Change Biology, 18*(3), 1016-1027.

Jensen, J. R. (2005). *Introductory digital image processing* (3rd ed.). Upper Saddle River, NJ: Pearson Prentice Hall.

Jensen, J. R. (2009). *Remote sensing of the environment: An earth resource perspective* (2nd ed.). Upper Saddle River, NJ: Pearson Prentice Hall.

Jones, H. G. (2013). *Plants and microclimate: A quantitative approach to environmental plant physiology*. Cambridge, UK: Cambridge University Press.

Kolb, K. J., & Davis, S. D. (1994). Drought tolerance and xylem embolism in co-occurring species of coastal sage and chaparral. *Ecology, 75*(3), 648-659. doi:10.2307/1941723

McGwire, K., Minor, T., & Fenstermaker, L. (2000). Hyperspectral mixture modeling for quantifying sparse vegetation cover in arid environments. *Remote Sensing of Environment, 72*(3), 360-374.

Meentemeyer, R. K., & Moody, A. (2000). Rapid sampling of plant species composition for assessing vegetation patterns in rugged terrain. *Landscape Ecology, 15*(8), 697-711.

Miller, P. C. (1979). Patterns of water use by shrubs in Southern California USA. *Forest Science, 25*(1), 84-98.

Miller, P. C. (1981). *Resource use by chaparral and matorral. A comparison of vegetation function in two mediterranean type ecosystems*. New York, NewYork: Springer-Verlag.

Mooney, H. A., & Dunn, E. L. (1970). Photosynthetic systems of Mediterranean climate shrubs and tress of California and Chile. *American Naturalist, 104*(939), 447-453. doi:10.1086/282679

Narvaez, N., Brosh, A., & Pittroff, W. (2010). Seasonal dynamics of nutritional quality of California chaparral species. *Animal Feed Science and Technology, 158*(1–2), 44-56. doi:http://dx.doi.org/10.1016/j.anifeedsci.2010.03.014

National Drought Mitigation Center. (2015). *United States Drought Monitor*. Retrieved from http://droughtmonitor.unl.edu/MapsAndData/DataTables.aspx?CA.

National Oceanic and Atmospheric Administration (NOAA). (2014, April 20th). Observed Precipitation. *California Nevada River Forecast Center*. Retrieved from http://www.cnrfc.noaa.gov/rainfall_data.php

Office of Environmental Health Hazard Assessment. (2013). *Indicators of Climate Change in California*. Retrieved from http://www.oehha.ca.gov/multimedia/epic/2013EnvIndicatorReport.html.

Paddock, W., Davis, S. D., Pratt, R. B., Jacobsen, A. L., Tobin, M. F., Lopez-Portillo, J., & Ewers, F. (2013). Factors determining mortality of adult chaparral shrubs in an extreme drought year in California. *Aliso, 31*(1), 49-57.

Parry, M. L. (2007). *Climate change 2007: Impacts, adaptation and vulnerability: Contribution of Working Group II to the fourth assessment report of the Intergovernmental Panel on Climate Change* (Vol. 4). Cambridge, UK: Cambridge University Press.

Parsons, D. J. (1976). Vegetation structure in the mediterranean scrub communities of California and Chile. *The Journal of Ecology*, 435-447.

Parsons, D. J., Rundel, P. W., Hedlund, R. P., & Baker, G. A. (1981). Survival of severe drought by a non-sprouting chaparral shrub. *American Journal of Botany, 68*(7), 973-979. doi:10.2307/2443229

Pavlik, B. M., Muick, P., Johnson, S., & Popper, M. (1991). *Oaks of California*. Los Olivos, CA: Cachuma Press.

Peters, A. J., Walter-Shea, E. A., Ji, L., Vina, A., Hayes, M., & Svoboda, M. D. (2002). Drought monitoring with NDVI-based standardized vegetation index. *Photogrammetric Engineering and Remote Sensing, 68*(1), 71-75.

Poole, D. K., & Miller, P. C. (1975). Water relations of selected species of chaparral and coastal sage communities. *Ecology, 56*(5), 1118-1128. doi:10.2307/1936151

Quinn, R. D., & Keeley, S. C. (2006). *Introduction to California chaparral* (Vol. 90). Berkeley, CA: University of California Press.

Rahimzadeh Bajgiran, P., Darvishsefat, A. A., Khalili, A., & Makhdoum, M. F. (2008). Using AVHRR-based vegetation indices for drought monitoring in the Northwest of Iran. *Journal of Arid Environments, 72*(6), 1086-1096.

Roberts, D. A., Green, R., & Adams, J. (1997). Temporal and spatial patterns in vegetation and atmospheric properties from AVIRIS. *Remote Sensing of Environment, 62*(3), 223-240.

Roberts, D. A. (1993). Green vegetation, nonphotosynthetic vegetation, and soils in AVIRIS data. *Remote Sensing of Environment, 44*(2-3), 255-269.

Roberts, D. A., Dennison, P. E., Morais, M., Gardner, M. E., Regelbrugge, J., & Ustin, S. L. (1999). *Mapping wildfire fuels using imaging spectrometry along the wildland urban interface.* Paper presented at the Proc. Joint Fire Sci. Conf. Workshop.

Roberts, D. A., Dennison, P. E., Peterson, S., Sweeney, S., & Rechel, J. (2006). Evaluation of Airborne Visible/Infrared Imaging Spectrometer (AVIRIS) and Moderate Resolution Imaging Spectrometer (MODIS) measures of live fuel moisture and fuel condition in a shrubland ecosystem in southern California. *Journal of Geophysical Research: Biogeosciences, 111*(G4), G04S02. doi:10.1029/2005JG000113

Roberts, D. A., Dennison, P. E., Roth, K. L., Dudley, K., & Hulley, G. (2015). Relationships between dominant plant species, fractional cover and Land Surface Temperature in a Mediterranean ecosystem. *Remote Sensing of Environment*(0).INCOMPLETE doi:http://dx.doi.org/10.1016/j.rse.2015.01.026

Roberts, D. A., Gardner, M., Church, R., Ustin, S., Scheer, G., & Green, R. O. (1998). Mapping chaparral in the Santa Monica Mountains using multiple endmember spectral mixture models. *Remote Sensing of Environment, 65*(3), 267-279.

Röder, A., Hill, J., Kuemmerle, T., del Barrio, G., Papanastasis, V. P., & Tsiourlis, G. M. (2009). Geomatics-based characterization of spatial and temporal trends in heterogeneous Mediterranean rangelands of Northern Greece. *Recent Advances in Remote Sensing and Geoinformation Processing for Land Degradation Assessment*, 281.

Roth, K. L., Dennison, P. E., & Roberts, D. A. (2012). Comparing endmember selection techniques for accurate mapping of plant species and land cover using imaging spectrometer data. *Remote Sensing of Environment, 127*(0), 139-152. doi:http://dx.doi.org/10.1016/j.rse.2012.08.030

Somers, B., & Asner, G. P. (2012). Hyperspectral time series analysis of native and invasive species in Hawaiian rainforests. *Remote Sensing, 4*(9), 2510-2529.

Somers, B., & Asner, G. P. (2013). Multi-temporal hyperspectral mixture analysis and feature selection for invasive species mapping in rainforests. *Remote Sensing of Environment, 136*, 14-27.

Somers, B., & Asner, G. P. (2014). Tree species mapping in tropical forests using multi-temporal imaging spectroscopy: Wavelength adaptive spectral mixture analysis. *International Journal of Applied Earth Observation and Geoinformation, 31*, 57-66.

Thompson, D. R., Gao, B.-C., Green, R. O., Roberts, D. A., Dennison, P. E., & Lundeen, S. (2015). Atmospheric correction for global mapping spectroscopy: ATREM advances for the HyspIRI preparatory campaign. *Remote Sensing of Environment,* 167, 64-77.

Tucker, C. J., Justice, C. O., & Prince, S. D. (1986). Monitoring the grasslands of the Sahel 1984-1985. *International Journal of Remote Sensing, 7*(11), 1571-1581.

Tucker, C. J., Vanpraet, C. L., Sharman, M. J., & Van Ittersum, G. (1985). Satellite remote sensing of total herbaceous biomass production in the senegalese sahel: 1980-1984. *Remote Sensing of Environment, 17*(3), 233-249.

Ustin, S. L., Roberts, D. A., Gamon, J. A., Asner, G. P., & Green, R. O. (2004). Using imaging spectroscopy to study ecosystem processes and properties. *BioScience,* *54*(6), 523-534.

Van Mantgem, P. J., & Stephenson, N. L. (2007). Apparent climatically induced increase of tree mortality rates in a temperate forest. *Ecology Letters, 10*(10), 909-916.

Vogelmann, J. E., Tolk, B., & Zhu, Z. (2009). Monitoring forest changes in the southwestern United States using multitemporal Landsat data. *Remote Sensing of Environment, 113*(8), 1739-1748.